PHYSICAL REVIEW B **96**, 161303(R) (2017)

Weak antilocalization induced by Rashba spin-orbit interaction in layered III-VI compound semiconductor GaSe thin films

Shoichi Takasuna,[1] Junichi Shiogai,[1,2] Shunichiro Matsuzaka,[3] Makoto Kohda,[1,4] Yutaka Oyama,[1] and Junsaku Nitta[1,4]

[1]*Department of Materials Science, Tohoku University, Sendai 980-8579, Japan*

[2]*Institute for Materials Research, Tohoku University, Sendai 980-8577, Japan*

[3]*Nanophoton R&D Center, Nanophoton Corporation, Osaka 565-0871, Japan*

[4]*Center for Spintronics Research Network, Tohoku University, Sendai 980-8579, Japan*

(Received 18 May 2017; revised manuscript received 11 September 2017; published 30 October 2017)

Magnetoconductance (MC) at low temperature was measured to investigate spin-related transport affected by spin-orbit interaction (SOI) in III-VI compound n-type GaSe thin films. Results reveal that MC shows weak antilocalization (WAL). Its temperature and gate voltage dependences reveal that the dominant spin relaxation is governed by the D'yakonov-Perel' mechanism associated with the Rashba SOI. The estimated Rashba SOI strength in GaSe is much stronger than that of III-V compound GaAs quantum wells, although the energy gap and spin split-off band in GaSe closely resemble those in GaAs. The angle dependence of WAL amplitude in the in-plane magnetic field direction is almost isotropic. This isotropy indicates that the strength of the Dresselhaus SOI is negligible compared with the Rashba SOI strength. The SOI effect in n-GaSe thin films differs greatly from those of III-V compound semiconductors and transition-metal dichalcogenides.

DOI: 10.1103/PhysRevB.96.161303

After the discovery of graphene, great attention has been devoted to transition-metal dichalcogenides (TMDs) for use as next-generation electronic materials because they have a band gap and intriguing graphenelike properties [1]. Recently, layered III-VI compound semiconductors MX (M = Ga, In and X = S, Se, Te) have emerged as promising candidates for use as ultrathin field effect transistors (FETs) [2] with high-mobility transport [3]. Transistor operation in single-layer GaS and GaSe has been demonstrated [4]. Because of the direct band gap, high performance of photodetectors has been achieved using atomic layered GaSe [5,6]. Optical spin dynamics in GaSe thin films were also investigated [7,8]. The quantum Hall effect and anomalous optical response were observed in atomically thin InSe with high electron mobility [3]. The band structure of layered III-VI compound semiconductors differs from that of TMDs. An almost direct band gap exists at the Γ point, depending on the number of layers [9]. The unusual distortion of the valence-band maximum is predicted to create an indirect band gap and singularity of density of states, which theoretically causes tunable magnetism in the p-type monolayer GaSe [10]. Occurrence of a topological insulator in layered GaSe and GaS is predicted by introducing tensile strain [11]. For these exotic phenomena, spin-orbit interaction (SOI) plays a necessary role in the topological phase transition and magnetic anisotropy.

The unit cell of a single GaSe layer and top view of GaSe shown in Figs. 1(a) and 1(b) have mirror reflection ($z \rightarrow -z$) symmetries. The electrical dipole moments with threefold rotational symmetry in the x-y plane presented in Fig. 1(c) induce Dresselhaus SOI [12], as expressed by the following equation with coefficient γ [13]:

$$H_D = \gamma\left(3k_x^2 - k_y^2\right)k_y\sigma_z. \tag{1}$$

As presented in Fig. 1(d), the Dresselhaus effective SOI field shows out-of-plane orientation with threefold rotational symmetry because the effective SOI field is given as $\vec{B}_{\rm eff} \propto \vec{p} \times \vec{E}$ with electron momentum $\vec{p}$ and in-plane dipole electric field $\vec{E}$. The form of Dresselhaus SOI is universal for all other bands, but with a different γ coefficient [13]. This Dresselhaus SOI-induced spin splitting in GaSe at the Γ point differs from the Zeeman-type spin splitting appearing at K points in TMDs [14]. It is noteworthy that the out-of-plane orientation of the effective magnetic field in III-VI layered semiconductors resembles the case of III-V GaAs [110] quantum wells (QWs), for which long spin-relaxation times have been observed [15]. In this case, weak antilocalization (WAL) is suppressed and weak localization (WL) appears in transport experiments because the acquired spin phases are identical in time-reversal interference paths under the unidirectional $\vec{B}_{\rm eff}$ condition.

In addition to the Dresselhaus SOI, the Rashba SOI [16] can be expected if there is structural inversion asymmetry at the interface between GaSe and substrate. The Rashba SOI field $\vec{B}_{\rm eff}$ is in-plane orientation with isotropic strength, as presented in Fig. 1(e). The total SOI Hamiltonian for GaSe thin films is expressed as shown below:

$$H_{\rm total} = \alpha(k_x\sigma_y - k_y\sigma_x) + \gamma\left(3k_x^2 - k_y^2\right)k_y\sigma_z. \tag{2}$$

However, the Rashba SOI effect in GaSe is not expected to be sufficiently strong to cause WAL because the energy gap $Eg = 2.0\,\text{eV}$ and spin split-off band $\Delta\text{so} = 0.34\,\text{eV}$ in GaSe [17] closely resemble $Eg = 1.5$ eV, $\Delta\text{so} = 0.34\,\text{eV}$ in GaAs [18]. The observation of WAL in two-dimensional (2D) GaAs is limited to less than 1 K, where the phase coherence length becomes greater than spin-relaxation length [19].

Although III-VI compound layer semiconductors have been investigated extensively, experimental studies of spin-related transport affected by SOI are very few. In this Rapid Communication, magnetotransport properties in GaSe thin films are investigated at low temperature. Surprisingly, the WAL is observed at relatively high temperature $T > 1$ K in our present GaSe thin films. This study was conducted to clarify the effect of SOI on spin-related transport, which is crucially

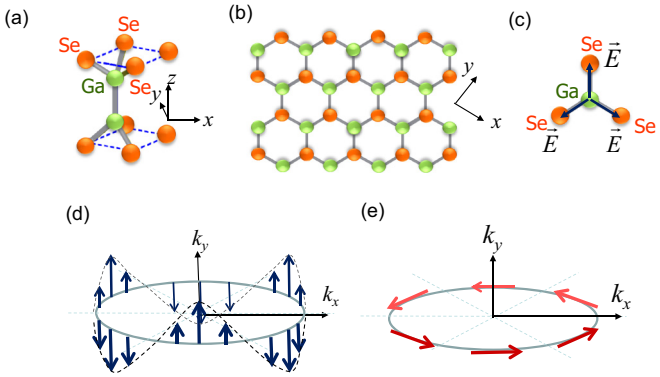

FIG. 1. (a) Perspective view of single-layer GaSe unit cell. (b) Top view of GaSe. Orange and green spheres respectively correspond to Se and Ga atoms. (c) Ga and Se atoms form a threefold rotational net in-plane electric dipole moment which is responsible for Dresselhaus SOI. (d) Momentum-dependent effective magnetic field induced by Dresselhaus SOI. Effective magnetic field points perpendicular to the plane, irrespective of momentum direction. (e) Rashba-SOI-induced effective magnetic field. The effective field direction is in-plane and perpendicular to the momentum direction. The strength of the effective field is isotropic.

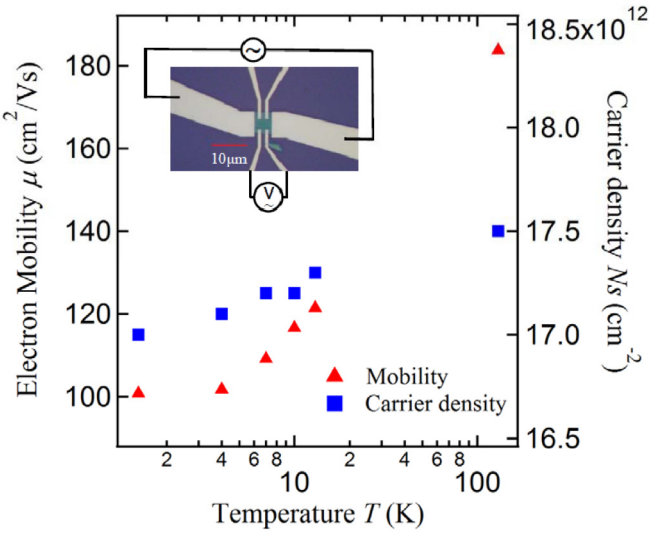

FIG. 2. Temperature dependence of electron mobility μ and carrier density N_s for device no. 1. μ and N_s are estimated from ρ_{xx} and ρ_{xy}. The inset presents a photograph of the fabricated multilayered GaSe device structure.

important for magnetism and topological phase transition in layered III-VI materials.

From a bulk GaSe sample grown by the Bridgman method, GaSe thin films were exfoliated using the mechanical cleavage method. These films were attached on cleaned p-doped Si/SiO_2 (300 nm, thermal oxidation) substrates. This SiO_2 oxide layer was used as a gate dielectric layer for a back-gate electrode (p-doped Si). The layer thickness of GaSe thin films was ascertained from color contrast in optical images of GaSe layers. The relation between color contrast and GaSe thickness was calibrated using atomic force microscopy and Raman spectroscopy. The Raman spectra revealed that the GaSe samples used in the experiment have an ε-type layer structure [20–22] (see Supplemental Material, Sec. 1). For four-probe measurements and Hall effect measurements, Ag electrodes serving as Ohmic contacts were defined on GaSe flakes using electron-beam lithography, as presented in the inset of Fig. 2.

The temperature dependence of carrier density N_s and mobility μ for device no. 1 with 10-nm-thick GaSe film is presented in Fig. 2. Carrier density N_s and mobility μ were estimated from longitudinal resistance ρ_{xx} and Hall resistance ρ_{xy}. We confirmed that the carriers in our present samples are *electrons* from the sign of Hall voltage and gate voltage dependence of ρ_{xy}. Actually, electron mobility μ decreases concomitantly with decreasing temperature T, although N_s remains almost constant. The temperature dependence of sheet conductance closely resembles the temperature dependence of μ. A similar temperature dependence of N_s and μ was observed for device no. 2 with 25-nm-thick GaSe. The decrease in μ at low temperature less than 100 K might be attributed to ionized impurity scattering, as reported in MoS_2 monolayer [23]. We consider that the high electron density and the reduction of mobility at low temperatures are related to the Se vacancy in our present samples.

A quantum interference effect such as WL is sensitive to phase coherence and spin relaxation. Actually, WL becomes WAL when spin-relaxation length ℓ_{SO} is shorter than phase coherence length ℓ_ϕ. In III-V compound QWs, WAL analysis has been used to estimate the SOI strength [24]. The WL and WAL analyses were applied to TMDs 2D materials such as MoS_2 [25], WSe_2 [14], and $MoSe_2$ [26] because ℓ_ϕ is longer than the thickness of their samples. In this work, we apply 2D WAL analysis to our GaSe thin films by treating GaSe thin films as 2D conductors. Magnetoconductance (MC) for device no. 1 was measured using a conventional lock-in method at low temperature T, as depicted in Fig. 3(a). MC data show strong temperature dependence and a conductance peak around a zero magnetic field with amplitude order of e^2/h. These features originate from WAL properties. It is noteworthy that no WAL behaviors were observed in thin and monolayer n-type MoS_2 [25,27], even if a strong SOI is expected. That is true probably because the intravalley scattering effect is dominant [28] and because the intra- and intervalley scatterings complicate the analysis.

Two possible reasons exist for the WAL: the Elliot-Yafet (EY) and D'yakonov-Perel' (DP) spin-relaxation mechanisms [29]. The EY spin-relaxation mechanism is associated with admixture of spin-up and -down states where spin and momentum are entangled by SOI. Therefore, momentum scattering events cause the spin-flip process. The DP spin-relaxation mechanism is fundamentally attributable to a motion-narrowing effect of spin precession induced by an effective magnetic field B_{eff}, which appears in spin splitting of a band with the lack of spatial inversion symmetry. Therefore, spin-relaxation time τ_{SO} is inversely proportional to momentum scattering time τ_{tr} for the DP mechanism, whereas τ_{SO} is proportional to τ_{tr} for the EY mechanism.

Experimentally measured WAL data are well reproduced by Iordanskii, Lyanda-Geller, and Pikus (ILP) theory [30] based on the DP mechanism. In Fig. 3(a), black solid curves are

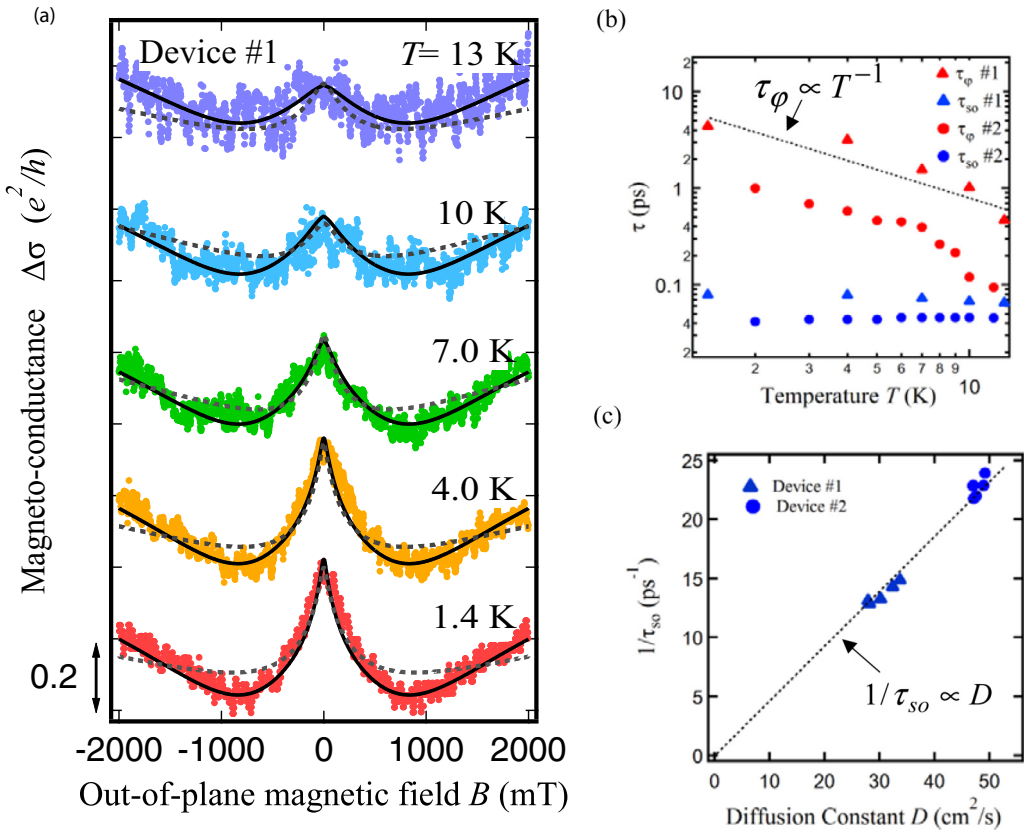

FIG. 3. (a) Magnetoconductance (MC) data for device no. 1 observed at low temperature. The MC data are well reproduced by weak antilocalization (WAL) analysis using ILP theory based on the DP spin-relaxation mechanism, as shown by solid curves. Dashed curves are analyzed using HLN theory based on the EY spin-relaxation mechanism. The ILP theory provides better agreement with the experiment. This result demonstrates that the DP mechanism is dominant over the EY mechanism. Theoretical fittings with ILP theory are used to extract spin-relaxation length ℓ_{SO} and phase coherence length ℓ_ϕ. (b) Temperature dependence of phase coherence time τ_ϕ and spin-relaxation time τ_{SO}. τ_ϕ and τ_{SO} are extracted from ℓ_ϕ and ℓ_{SO} with the assumption of $m^* = 0.25$. The dotted line shows $\tau_\phi \propto T^{-1}$ dependence for comparison. (c) Relation between spin-relaxation rate ${\tau_{SO}}^{-1}$ and diffusion constant D for devices no. 1 and no. 2. Diffusion constant D is estimated from the temperature dependence of the electron carrier density and mobility. The dotted line is a guide showing ${\tau_{SO}}^{-1} \propto D$.

obtained from analysis using the ILP theory. The ILP analysis including only the Rashba term was used as described in Ref. [24]. The Hikami, Larkin, and Nagaoka (HLN) theory [31] with an assumption of the EY mechanism failed to reproduce the WAL data, as shown by the dashed line in Fig. 3(a). The temperature dependence of τ_ϕ and τ_{SO} extracted from the ILP analysis is depicted in Fig. 3(b), showing that τ_ϕ is almost inversely proportional to T in a higher temperature region, but it saturates at lower temperatures. The values of τ_ϕ and τ_{SO} are extracted from ℓ_ϕ and ℓ_{SO} values with an assumption of $m^* = 0.25$, as discussed below. The $\tau_\phi \propto T^{-1}$ dependence, which is attributable to electron-electron scattering, has been reported in dirty 2D metals [32]. Temperature dependences of ℓ_ϕ and ℓ_{SO} values for devices 1 and 2 are presented in [33].

To extract τ_{SO} from $\ell_{SO} = \sqrt{D\tau_{SO}}$, one must ascertain the value of effective mass m^* and diffusion constant D of GaSe layers. Recently, the effective mass of InSe thin film was found to be $m^* = 0.14-0.17$ from the temperature dependence of Shubnikov–de Haas oscillation amplitude [3]. However, the data of effective mass in GaSe are extremely limited. Therefore, $m^* = 0.25$ is assumed by considering the ratio of energy gap between InSe and GaSe [34]. Figure 3(c) represents the relation between spin-relaxation rate ${\tau_{SO}}^{-1}$ and diffusion constant D for devices 1 and 2. The values of D were estimated from the temperature dependence of N_s and μ with the assumption of $m^* = 0.25$. The linear relation between ${\tau_{SO}}^{-1}$ and D among both samples with different thickness indicates the same origin of SOI. Here, D is proportional to τ_{tr}. This result demonstrates that the DP spin-relaxation mechanism is dominant in the present GaSe samples. The experimentally observed WAL cannot be explained if only the Dresselhaus SOI exists as given by Eq. (1). Therefore, we infer that the Rashba SOI causes WAL, and that is attributable to the origin of the DP spin-relaxation mechanism. The Rashba SOI originates from structural inversion asymmetry. Therefore, the results presented above indicate that the interface between GaSe and the substrate plays an important role.

If the Rashba SOI plays a role in the present GaSe thin films, one can expect gate control of the Rashba parameter. The back-gate voltage V_{BG} dependence of WAL for device no. 2 [35] was measured at $T = 2$ K. The WAL data and their analysis using the ILP theory shown by black curves are presented in Fig. 4(a). The negative magnetoconductance region, which characterizes the WAL strength shown by arrows, grows by positively increasing V_{BG}. The V_{BG} dependence of ℓ_ϕ, ℓ_{SO}

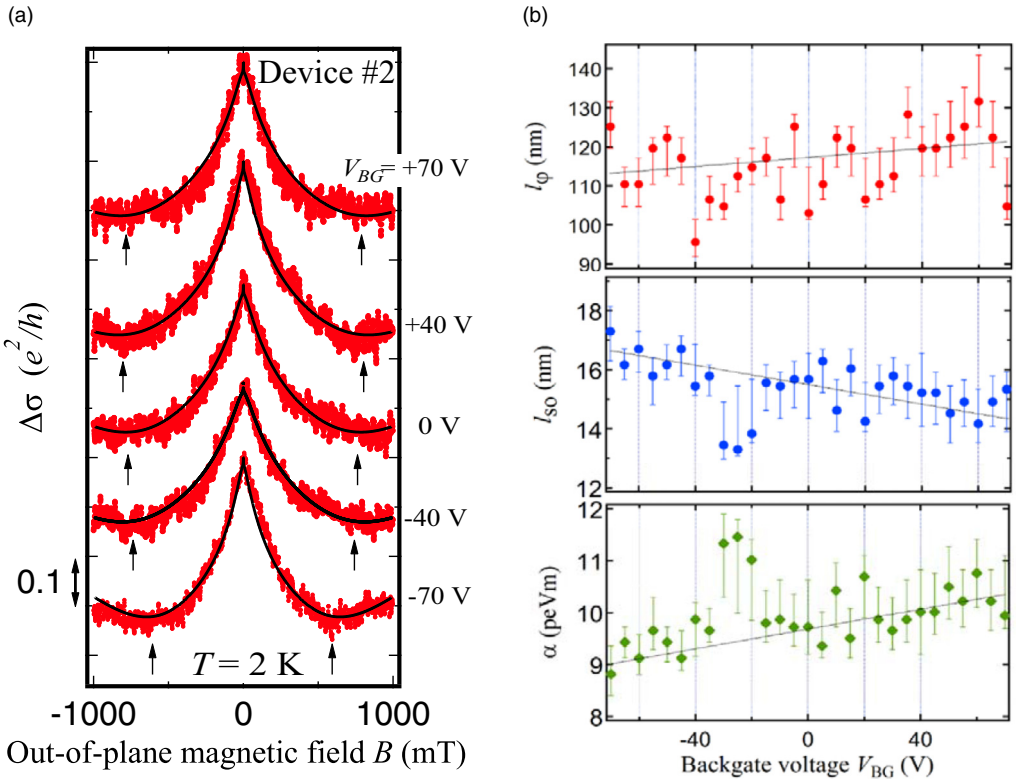

FIG. 4. (a) Back-gate voltage V_{BG} dependence of WAL measured at $T = 2$ K for device no. 2. Arrows indicate magnetoconductance minimum fields, corresponding to the strength of WAL. Solid curves show results of analysis using the ILP theory to extract Rashba SOI parameter α. (b) V_{BG} dependence of phase coherence length ℓ_ϕ, spin-relaxation length ℓ_{SO}, and Rashba SOI strength α.

and Rashba SOI α extracted from the ILP theory analysis are portrayed in Fig. 4(b). The ℓ_ϕ is increased slightly with increasing V_{BG}, although ℓ_{SO} is decreased. The reduction of $\ell_{SO} = \sqrt{D\tau_{SO}}$ with increasing V_{BG} cannot be explained by the modulation of D because D increases with V_{BG} and N_s. The result portrayed in Fig. 4(b) reports a gate-controlled Rashba SOI strength $\alpha = \alpha_{\rm SO}\langle E\rangle$, which is estimated by the following relation:

$$\alpha = \frac{\hbar^2}{2\ell_{so}m^*}. \tag{3}$$

Given the assumption of $m^* = 0.25$, the Rashba SOI can be estimated as $\alpha \sim 10 \times 10^{-12}$ eV m, which is the same order of InGaAs QWs [36] and which is 1 order higher than that of GaAs QWs [37]. The Rashba SOI strength of $\alpha \approx 2.5 \times 10^{-12}$ eV m is still high, even with an assumption of very large effective mass of $m* = 1.1$, which is reported in chlorine-doped n-GaSe [38]. In III-V compound semiconductors, the Rashba coefficient $\alpha_{\rm SO}$ depends not only on spin splitting in the valence band but also on the energy gap, and it is shown theoretically that the coefficient $\alpha_{\rm SO}$ is enhanced considerably with the decrease in the energy gap [39]. It is noteworthy that the Rashba SOI strength of GaSe is rather high if one considers the large band-gap energy of 1.2–2.0 eV in ε-GaSe [17].

The modulation of Rashba SOI $\alpha = \alpha_{\rm SO}\langle E\rangle$ by V_{BG} is relatively small (∼10%) even with large V_{BG} application. It is expected that the change in the electric field $\langle E\rangle$−induced potential profile of the GaSe channel is small because the modulation of carrier density by the back-gate voltage is limited to ∼15% of total carrier density [40].

In the ε-type GaSe, the dipole electric moments between two adjacent monolayers are parallel [17]; therefore, the Dresselhaus SOI is not cancelled out in multilayers. A final question is whether the Dresselhaus SOI in the present system is negligible or not. Additional analyses were conducted using an in-plane magnetic field. When the total SOI field strength in the system is anisotropic because of the coexistence of both Rashba and Dresselhaus SOIs, we can expect the anisotropic WAL as a function of the in-plane magnetic field direction. This anisotropic WAL originates from spin-dependent additional dephasing caused by competition between the SOI field and the Zeeman field [41]. The anisotropy is also expected even if the Dresselhaus SOI effective field is oriented along the z direction, such as [110] QWs in III-V compound semiconductors. The WAL amplitude is maximal when the in-plane field is parallel to the direction of the maximum total SOI field [41].

MC for device no. 2 was measured at $T = 2$ K and $V_{BG} = 0$ V under a constant in-plane magnetic field $B_{//} = 1$ T as presented in Fig. 5(a). The amplitude of the WAL $\Delta\sigma_{\rm peak}$ is suppressed by $B_{//}$, but WAL is still clearly observed. In our GaSe thin films, strong reduction of ℓ_ϕ by an in-plane magnetic field shows that the interlayer coupling is not negligible [42]. The same MC measurements were performed by rotating the in-plane magnetic field direction with an angle step of 5 deg. Figure 5(b) presents a color plot for the in-plane field angle dependence of WAL. To clarify it, the polar plot for $\Delta\sigma_{\rm peak}$

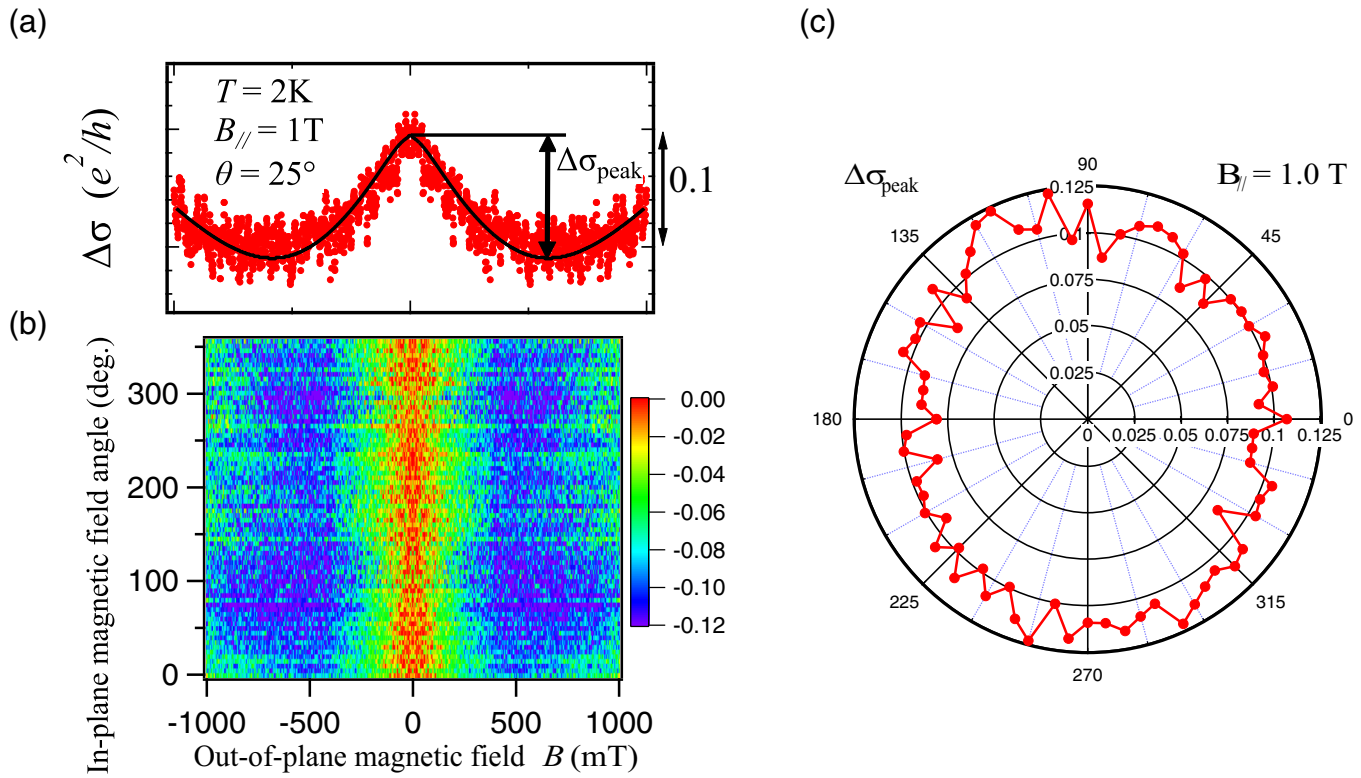

FIG. 5. (a) MC for device no. 2 measured at $T = 2$ K and $V_{BG} = 0$ V under constant in-plane magnetic field $B_{//} = 1$ T. The amplitude of WAL is defined as $\Delta\sigma_{peak}$. (b) Color plot for the in-plane field angle dependence of WAL. WAL data were measured by rotating the direction of in-plane magnetic field $B_{//} = 1$ T with the angle step of 5 deg. The current direction is about -50 deg offset from the in-plane magnetic field direction of $\theta = 0$ deg. (c) Polar plot of WAL amplitude $\Delta\sigma_{peak}$ as a function of the in-plane field direction.

is presented in Fig. 5(c). The polar plot appears to be nearly isotropic. Anisotropic $\Delta\sigma_{peak}$ amplitude becomes maximum when the Zeeman field is comparable to the SO field. Because the obtained Rashba SO coefficient is around 10^{-11} eV m, which corresponds to 10 T for the SO field, the in-plane magnetic field is too small to modulate the WAL amplitude drastically by additional spin-dependent dephasing. Recent *ab initio* calculation [17] shows that the Dresselhaus SOI in the GaSe conduction band is independent of the layer thickness and is weaker than that of GaAs, which holds a few teslas for the SO field. This experimentally obtained angle dependence indicates that the Rashba SOI strength is dominant over the Dresselhaus SOI, which is consistent with *ab initio* calculations.

In summary, the well-established WAL analysis used in III-V compound semiconductors was applied to layered III-VI compound GaSe films. The WAL, which is not expected from the Dresselhaus SOI in GaSe, was observed at $T > 1$ K. The WAL analysis reveals that the dominant spin-relaxation mechanism is attributed to the DP mechanism associated with the Rashba SOI. Surprisingly, the Rashba SOI strength is greater than that in GaAs QWs. Dependence of the WAL amplitude on the in-plane magnetic field direction is almost isotropic, indicating that the strength of the Dresselhaus SOI is negligible compared with the Rashba SOI strength. The SOI effects in these GaSe thin films differ from those observed in III-V compound semiconductors and TMDs. These results shed light on the SOI-effect-induced intriguing phenomena in III-VI compound semiconductor thin films. Moreover, GaSe thin films are expected to provide a fruitful playground of spin orbitronics [43]. All-GaSe spin-field-effect transistors are possible by combining gate-tunable magnetism [10] and Rashba SOI in GaSe.

This work was supported by Grants-in-Aid for Scientific Research (No. 15H05699) from the Japan Society for the Promotion of Science.

[1] Q. H. Wang, K. Kalantar-Zadeh, A. Kis, J. N. Coleman, and M. S. Strano, Nat. Nanotechnol. **7**, 699 (2013).
[2] S. Sucharitakul *et al.*, Nano. Lett. **15**, 3815 (2015).
[3] D. A. Bandurin *et al.*, Nat. Nanotechnol. **12**, 223 (2016).
[4] D. J. Late, B. Liu, J. Luo, A. Yan, H. S. S. R. Matte, M. Grayson, C. N. R. Rao, and V. P. Dravid, Adv. Mater. **24**, 3549 (2012).
[5] P. Hu, Z. Wen, L. Wang, P. Tan, and K. Xiao, ACS Nano **6**, 5988 (2012).
[6] S. Lei, L. Ge, Z. Liu, S. Najmaei, G. Shi, G. You, J. Lou, R. Vajtai, and P. M. Ajayan, Nano Lett. **13**, 2777 (2013).
[7] Y. Tang, W. Xie, K. C. Mandal, J. A. McGuire, and C. W. Lai, J. Appl. Phys. **118**, 113103 (2015).
[8] Y. Tang, W. Xie, K. C. Mandal, J. A. McGuire, and C. W. Lai, Phys. Rev. B **91**, 195429 (2015).
[9] Y. Ma, Y. Dai, M. Guo, L. Yu, and B. Huang, Phys. Chem. Chem. Phys. **15**, 7098 (2013).

[10] T. Cao, Z. Li, and S. G. Louie, Phys. Rev. Lett. **114**, 236602 (2015).
[11] Z. Zhu, Y. Cheng, and U. Schwingenschloegl, Phys. Rev. Lett. **108**, 266805 (2012).
[12] G. Dresselhaus, Phys. Rev. **100**, 580 (1955).
[13] P. Li and I. Appelbaum, Phys. Rev. B **92**, 195129 (2015).
[14] H. Yuan, M. S. Bahramy, K. Morimoto, S. Wu, K. Nomura, B. J. Yang, H. Shimotani, R. Suzuki, M. Toh, C. Kloc, X. Xu, R. Arita, N. Nagaosa, and Y. Iwasa, Nat. Phys. **9**, 563 (2013).
[15] Y. Ohno, R. Terauchi, T. Adachi, F. Matsukura, and H. Ohno, Phys. Rev. Lett. **83**, 4196 (1999).
[16] E. I. Rashba, Fiz. Tverd. Tela (Leningrad) **2**, 1224 (1960) [Sov. Phys. Solid State **2**, 1109 (1960)].
[17] D. T. Do, S. D. Mahanti, and C. W. Lai, Sci. Rep. **5**, 17044 (2015).
[18] R. Winkler, in *Spin-orbit Coupling Effects in Two-Dimensional Electron and Hole Systems*, edited by P. Woelfle, Springer Tracts in Modern Physics Vol. 191 (Springer, Berlin, 2003).
[19] J. B. Miller, D. M. Zumbühl, C. M. Marcus, Y. B. Lyanda-Geller, D. Goldhaber-Gordon, K. Campman, and A. C. Gossard, Phys. Rev. Lett. **90**, 076807 (2003).
[20] See Supplemental Material at http://link.aps.org/supplemental/10.1103/PhysRevB.96.161303 for Raman spectrum.
[21] A. M. Kulibekov, H. P. Olijnyk, A. P. Jephcoat, Z. Y. Salaeva, S. Onari, and K. R. Allakheverdiev, Phys. Status Solidi B **235**, 517 (2003).
[22] D. J. Late, B. Liu, H. S. S. R. Matte, C. N. R. Rao, and V. P. Dravid, Adv. Funct. Mater. **22**, 1894 (2012).
[23] B. Radisavljevic and A. Kis, Nat. Mater. **12**, 815 (2013).
[24] T. Koga, J. Nitta, T. Akazaki, and H. Takayanagi, Phys. Rev. Lett. **89**, 046801 (2002).
[25] A. T. Neal, H. Liu, J. Gu, and P. D. Ye, ACS Nano **7**, 7077 (2013).
[26] Y. J. Zhang, W. Shi, J. T. Ye, R. Suzuki, and Y. Iwasa, Phys. Rev. B **95**, 205302 (2017).
[27] H. Schmidt, I. Yudhistira, L. Chu, A. H. Castro Neto, B. Ozyilmaz, S. Adam, and G. Eda, Phys. Rev. Lett. **116**, 046803 (2016).
[28] H. Z. Lu, W. Yao, D. Xiao, and S. Q. Shen, Phys. Rev. Lett. **110**, 016806 (2013).
[29] M. I. D'yakonov and V. I. Perel', Phys. Lett. A **35**, 459 (1971).
[30] S. V. Iordanskii, Y. B. Lyanda-Geller, and G. E. Pikus, Pis'ma Zh. Eksp. Teor. Fiz. **60**, 199 (1994) [JETP Lett. **60**, 206 (1994)].
[31] S. Hikami, A. I. Larkin, and Y. Nagaoka, Prog. Theor. Phys. **63**, 707 (1980).
[32] H. Fukuyama and E. Abrahams, Phys. Rev. B **27**, 5976 (1983).
[33] See Supplemental Material at http://link.aps.org/supplemental/10.1103/PhysRevB.96.161303 for weak antilocalization analysis based on HLN and ILP theories.
[34] A. Segura, J. Bouvier, M. V. Andres, F. J. Manjon, and V. Munoz, Phys. Rev. B **56**, 4075 (1997).
[35] Device no. 1 was damaged during the measurements. The voltage leads for ρ_{xy} for device no. 2 were also damaged during back-gate voltage dependence of WAL measurements. Therefore, we can only measure the ρ_{xx} and its magnetoconductance for device no. 2. The broken Hall voltage leads did not affect the ρ_{xx} values.
[36] J. Nitta, T. Akazaki, H. Takayanagi, and T. Enoki, Phys. Rev. Lett. **78**, 1335 (1997).
[37] L. Meier, G. Salis, I. Shorubalko, E. Gini, S. Schon, and K. Ensslin, Nat. Phys. **3**, 650 (2007).
[38] G. Micocci, A. Serra, and A. Tepore, J. Appl. Phys. **82**, 2365 (1997).
[39] E. A. de Andrada e Silva, G. C. La Rocca, and F. Bassani, Phys. Rev. B **55**, 16293 (1997).
[40] See Supplemental Material at http://link.aps.org/supplemental/10.1103/PhysRevB.96.161303 for gate voltage dependence of carrier density for device no. 2.
[41] A. G. Malshukov, V. A. Froltsov, and K. A. Chao, Phys. Rev. B **59**, 5702 (1999).
[42] See Supplemental Material at http://link.aps.org/supplemental/10.1103/PhysRevB.96.161303 for extracted characteristic transport parameters from ILP analysis.
[43] A. Manchon, H. C. Koo, J. Nitta, S. M. Frolov, and R. A. Duine, Nat. Mater. **14**, 871 (2015).